Biochemical and Biophysical Research Communications 456 (2015) 238–244

Contents lists available at ScienceDirect

Biochemical and Biophysical Research Communications

journal homepage: www.elsevier.com/locate/ybbrc

Arabidopsis dynamin-related proteins, DRP2A and DRP2B, function coordinately in post-Golgi trafficking

Jiahe Huang [a], Masaru Fujimoto [a], Masayuki Fujiwara [b], Yoichiro Fukao [b], Shin-ichi Arimura [a,c], Nobuhiro Tsutsumi [a,d,*]

[a] Laboratory of Plant Molecular Genetics, Graduate School of Agricultural and Life Sciences, The University of Tokyo, 1-1-1 Yayoi, Bunkyo-ku, Tokyo 113-8657, Japan
[b] Plant Global Education Project, Graduate School of Biological Sciences, Nara Institute of Science and Technology, 8916-5 Takayama, Ikoma, Nara 630-0192, Japan
[c] Japan Science and Technology Agency (JST), PRESTO, 4-1-8 Honcho, Kawaguchi, Saitama 332-0012, Japan
[d] Japan Science and Technology Agency (JST), CREST, 4-1-8 Honcho, Kawaguchi, Saitama 332-0012, Japan

ARTICLE INFO

Article history:
Received 13 November 2014
Available online 22 November 2014

Keywords:
Dynamin-related protein
Arabidopsis
DRP2
Post-Golgi trafficking

ABSTRACT

Dynamin-related proteins (DRPs) are large GTPases involved in a wide range of cellular membrane remodeling processes. In *Arabidopsis thaliana*, two paralogous land plant-specific type DRPs, DRP2A and DRP2B, are thought to participate in the regulation of post-Golgi trafficking. Here, we examined their molecular properties and functional relationships. qRT-PCR and GUS assays showed that DRP2A and DRP2B were expressed ubiquitously, although their expressions were strongest around root apical meristems and vascular bundles. Yeast two-hybrid, bi-molecular fluorescent complementation, and co-immunoprecipitation mass spectrometry analyses revealed that DRP2A and DRP2B interacted with each other. In observations with confocal laser scanning microscopy and variable incidence angle fluorescent microscopy, fluorescent fusions of DRP2A and DRP2B almost completely co-localized and were mainly localized to endocytic vesicle formation sites of the plasma membrane, clathrin-enriched *trans*-Golgi network and the cell plate in root epidermal cells. Treatments with wortmannin, an inhibitor of phosphatidylinositol 3-/4-kinases, latrunculin B, an inhibitor of actin polymerization, and oryzalin, an inhibitor of microtubule polymerization, increased the resident time of DRP2A and DRP2B on the plasma membrane. These results show that DRP2A and DRP2B function coordinately in multiple pathways of post-Golgi trafficking in phosphatidylinositol 3- or 4-kinase and cytoskeleton polymerization-dependent manners.
© 2014 Elsevier Inc. All rights reserved.

1. Introduction

Dynamin-related proteins (DRPs) are multidomain GTPases regulating membrane fission, fusion, and tubulation during diverse cellular activities such as endocytosis, cytokinesis, vacuolar sorting, fission and fusion of mitochondria, biogenesis of peroxisomes, and the maintenance of endoplasmic reticulum morphology [1,2]. DRPs are found in a broad range of eukaryotes and different DRPs usually have distinct cellular functions. Presently, the best characterized DRP is the authentic dynamin, which acts in clathrin-mediated post-Golgi trafficking in animal cells. During the formation of endocytic vesicles, dynamins are thought to form a ring or spiral polymer around the neck of an invaginated membrane and pinch off the bud in a GTP hydrolysis-dependent manner [3].

Dynamin contains five distinct domains: a GTPase domain whose GTP hydrolysis causes its own intramolecular conformational change, a middle domain that mediates dimerization during self-assembly, a GTPase-effector domain (GED) that modulates GTPase activity, a pleckstrin homology (PH) domain that participates in membrane bending or breakdown through the association of phosphatidylinositol-4,5-bisphosphate (PtdIns(4,5)P_2) and a proline-rich domain (PRD) that interacts with Src homology 3 (SH3) domain-containing proteins to recruit dynamin at vesicle formation sites [4]. The former three domains are conserved among almost all DRPs. However, DRPs with the latter two domains have been found only in animals and land plants. Most

Abbreviations: BiFC, bi-molecular fluorescent complementation; CLSM, confocal laser scanning microscopy; CoIP-MS, co-immunoprecipitation mass spectrometry; DRP, dynamin-related protein; GED, GTPase-effector domain; Lat B, latrunculin B; ORY, oryzalin; PH, pleckstrin homology; PI, phosphoinositide; PM, plasma membrane; PRD, proline-rich domain; PtdIns, phosphatidylinositol; Rr, Pearson's correlation coefficient; SH3, Src homology 3; TGN, *trans*-Golgi network; VIAFM, variable incidence angle fluorescent microscopy; Wm, wortmannin; Y2H, yeast two-hybrid.

* Corresponding author at: Laboratory of Plant Molecular Genetics, Graduate School of Agricultural and Life Sciences, The University of Tokyo, 1-1-1 Yayoi, Bunkyo-ku, Tokyo 113-8657, Japan. Fax: +81 3 5841 5183.
E-mail address: atsutsu@mail.ecc.u-tokyo.ac.jp (N. Tsutsumi).

http://dx.doi.org/10.1016/j.bbrc.2014.11.065
0006-291X/© 2014 Elsevier Inc. All rights reserved.

land plants have six types of DRPs (DRP1-DRP4, DRP5A, and DRP5B) [5], two of which (DRP1 and DRP2) have been reported to participate in post-Golgi trafficking [6].

In *Arabidopsis thaliana*, DRP1 subfamily consists of five members, DRP1A to DRP1E. DRP1A, DRP1C and DRP1E are expressed and mainly function in post-Golgi trafficking including clathrin-mediated endocytosis, which underlies cell expansion and cell plate formation [7]. DRP1A and DRP1C localize to the leading edge of the cell plate as well as the plasma membrane (PM). The phenotypes of *drp1* mutants include aberrant cell plate biogenesis, abnormal polarized cell expansion, altered cell wall composition, and decreased endocytosis. DRP1A is closely associated with auxin efflux carrier PIN-FORMED proteins [8]. DRP1 subfamily proteins lack a PH domain and a PRD. To our knowledge, the genomes of almost all green plants including algae have *DRP1* genes.

A. thaliana has two paralogous DRP2s, DRP2A and DRP2B, which have high amino acid sequence identity (92%). DRP2A and DRP2B localize to the leading edge of the forming cell plate, *trans*-Golgi network (TGN) and the PM [7,9]. The expression of dominant-negative DRP2A and DRP2B causes defects in root hair development [10]. The *drp2adrp2b* double mutant shows gametophyte-lethal phenotypes [11]. DRP2 subfamily proteins contain a PH domain and a PRD, whose organizations are similar to those of dynamin. Although DRP2s have structural similarities to animal dynamins, they are found only in land plants [12].

We have reported that DRP2B and DRP1A interact and co-localize on the PM, which indicates that they cooperate in vesicle formation in post-Golgi trafficking [9]. However, the molecular functions of DRP2s are not as well known as those of DRP1s. Here, we investigated four aspects of DRP2A and DRP2B: (i) whether their spatial expression patterns are similar or distinct, (ii) whether they form hetero-oligomers to co-assemble, (iii) which post-Golgi organelle do they localize in, and (iv) what molecules control their localizations.

2. Materials and methods

2.1. Plant materials and growth conditions

Arabidopsis plants (*A. thaliana*, ecotype *Columbia-0*) and tobacco plants (*Nicotiana benthamiana*, ecotype *SR-1*) were grown on jiffy pellets (Jiffy Products) or 1× Murashige Skoog (MS) solid medium [13] at 22 °C under continuous light. T-DNA insertion mutants were provided by the Arabidopsis Biological Resource Center (Ohio State University). Transgenic plants expressing DRP2B-GFP and DRP3B-mKO were generated as described previously [9,14]. Transgenic plants harboring *DRP2Apro:GUS, DRP2Bpro:GUS, DRP2A-GFP* and *DRP2B-TagRFP* were generated by floral dipping-mediated transformation with *Agrobacterium tumefaciens* strain C58C1. Transgenic plants expressing mRFP-ARA7 and ST-mRFP were gifts from Dr. T. Ueda, Dr. T. Uemura (The University of Tokyo) and Dr. K. Shoda (RIKEN). Transgenic plants that expressed combinations of GFP, TagRFP, mRFP and mKO fusions were generated by cross-pollination, and F1 generations were used for microscopic observations.

2.2. Construction of plasmids

Expressed sequence tag clones of *DRP2A* (GenBank accession no. AV529341) and *DRP2B* (GenBank accession no. AV528687) were obtained from Kazusa DNA Research Institute (Japan). Vectors for yeast two-hybrid assay and plant binary vectors harboring *DRP2A*, *DRP2B* and their promoters were constructed with In-Fusion HD cloning kit (Clontech) and Gateway cloning technology (Life technologies), respectively. Oligonucleotide primers used for plasmid construction are presented in Table S1.

To make binary vectors expressing GUS under the control of *DRP2A* and *DRP2B* promoters, the genomic DNA regions upstream of the ATG initiation codon of *DRP2A* and *DRP2B* (1545 bp and 1436 bp, respectively) were cloned into pHGWFS7 via pENTR/D-TOPO subcloning [15].

To make a binary vector for *DRP2A:GFP* expressed by *DRP2A*'s promoter, the *DRP2A* promoter and ORF were fused by PCR with synthetic overlapped primers. The resulting fragment of *DRP2A-pro:DRP2A* was cloned into pBGWF7 via pENTR/D-TOPO subcloning [15].

To make a binary vector for DRP2B-TagRFP expressed by own promoter, the fragment of *DRP2Bpro:DRP2B* established previously [6], was transferred to pGWB659 [16].

To make plasmids for bi-molecular fluorescent complementation assay, ORFs of DRP2A, DRP2B and DRP3A were introduced to pDEST-VYNE(R)^{GW} and pDEST-VYCE(R)^{GW} via pENTR/D-TOPO subcloning [17].

To make plasmids for yeast two-hybrid assay, ORFs of DRP2A, DRP2B and DRP3A were cloned into pGADT7 and pGBKT7, which harbor the gene encoding activation domain (AD) and binding domain (BD) of GAL4, by In-Fusion HD system with gene-specific primers containing EcoRI and BamHI restriction sites.

2.3. qRT-PCR

Total RNA was extracted from plants with an RNeasy Plant Mini Kit (QIAGEN). After DNase I treatment (Ambion), RNA was used for RT-PCR using SuperScript® III Reverse Transcriptase (Invitrogen). To quantify *DRP2A*, *DRP2B* and *ACT8* expression, real-time PCR was performed using 7300 Real-Time PCR System (Applied Biosystems) with Premix Ex Taq (Probe qPCR) and Dual Labeled TaqMan probes (FAM-TAMRA) (TaKaRa Bio). Each gene expression value is the average of three independent qPCR assays. Expression levels of *DRP2A* and *DRP2B* were normalized to those of *ACT8*. Primers and probes for each gene are listed in Table S1.

2.4. Histological analysis of GUS activity

Samples were fixed via immersion in 90% (v/v) ice-cold acetone overnight, rinsed twice with 100 mM sodium phosphate, incubated in GUS staining solution (50 mM sodium phosphate, pH 7.0, 10 mM EDTA, 0.5 mM ferrocyanide, 0.1% [v/v] Triton X-100, and 0.5 mg/mL 5-bromo-4-chloro-3-indolyl-beta-D-glucuronic acid) at 37 °C, incubated in ethanol-acetic acid, cleared in Hoyer's medium (7.5 g gum arabic, 100 g chloral hydrate, 5 ml glycerol in 30 ml water) and observed under a microscope (ECLIPSE E600, Nikon) with a CCD camera (DS-Ri1, Nikon) controlled by NIS-Elements (Nikon). The acquired images were prepared with Photoshop CS5 (Adobe).

2.5. Confocal laser scanning microscopy (CLSM)

CLSM observations were conducted with C1Si confocal microscope (Nikon) and LSM780 confocal microscope (Carl Zeiss), with oil immersion lenses (N.A. = 1.40, ×63 or ×100, respectively). In both systems, 488-nm Ar/Kr lasers were used for the excitation of GFP and Venus. 561-nm diode lasers were used for the excitation of mKO, mRFP, TagRFP, and autofluorescence. Emission signals were detected using a 515/30-nm filter for GFP and Venus, a 590/70-nm filter for mKO, TagRFP, and mRFP, and a 650-nm long-pass filter for autofluorescence. The acquired images were prepared with Photoshop CS5 (Adobe), and were analyzed by Image-pro plus 4.0 (Media Cybernetics).

2.6. Variable incidence angle fluorescent microscopy (VIAFM)

VIAFM observations were performed as described previously [6]. All images were acquired via an Eclipse Ti (Nikon) with a Zyla 4.2sCMOS camera (Ander) controlled by NIS-Elements (Nikon). The images were prepared with Photoshop CS5 (Adobe) and analyzed with Image-pro plus 4.0 (Media Cybernetics).

2.7. Yeast two-hybrid (Y2H) assay

Paired plasmids of pGADT7 and pGBKT7 harboring DRP2A, DRP2B, and DRP3A were transformed into *Saccharomyces cerevisiae* strain Y2HGold (Clontech). Y2HGold was deficient in producing Leu, Trp, His, and Adenin. Transformants were selected on SD/−Leu/−Thr plates (synthetic defined plates lucking Leu and Trp). The interactions were examined after 2 days of growth on SD/−Leu/−Trp/−His.

2.8. Bi-molecular fluorescent complementation (BiFC) assays

Three-week-old *N. benthamiana* plants were used for Agrobacterium-infiltrated transient expression. Vectors for the expression of nVenus or cVenus (nVenus: N-terminal 173 residues of Venus, cVenus: C-terminal 84 residues of Venus) fusions of DRP2A, DRP2B, and DRP3A were introduced into *A. tumefaciens* strain C58C1. Each transformant was cultured in 5 mL YEB medium with 50 μg/mL rifampicin, 10 μg/mL Gentamicin, 50 μg/mL Kanamycin at 28 °C overnight. Agrobacterium cells were collected and resuspended in infiltration buffer (10 mM MES, 10 mM $MgCl_2$, and 0.15 mM acetosyringone). Resuspended Agrobacterium cells were infiltrated into leaves of *N. benthamiana* with syringes. For co-expression of proteins, bacterial strains with different constructs were mixed before inoculation. Samples were observed 48 h after the infiltration by CLSM.

2.9. Co-immunoprecipitation mass spectrometry (CoIP-MS) analysis

Approximately 0.7 g of 10-day-old Arabidopsis seedlings were homogenized with sea sand in 1 mL of buffer (50 mM Tris-HCl, pH 7.5, 400 mM sucrose, 1% (v/v) Triton X-100, a complete mini EDTA free protease inhibitor cocktail (Roche), 150 mM NaCl, 5 mM $CaCl_2$, and 5 mM $MgCl_2$). The samples were centrifuged at 5000×*g* for 15 min at 4 °C and the supernatants were centrifuged again at 20,000×*g* for 15 min at 4 °C. The supernatants were immunoprecipitated with μMACS Anti-GFP Beads (Miltenyi Biotec), and separated by SDS-PAGE. The immunoprecipitates were prepared and examined by mass spectrometry as described previously [18].

2.10. Inhibitor treatments

10-day-old seedlings were cultured in 1× MS liquid medium with each inhibitor for 1 h (10 μM oryzalin and 50 μM latrunculin B) or 2 h (50 μM wortmannin). Seedlings treated with DMSO (1% for oryzalin and wortmannin, and 2% for latrunculin B) were used as controls.

3. Results

3.1. DRP2A and DRP2B exhibit similar expression patterns in A. thaliana

DRP2A and *DRP2B* mRNAs were detected in wild-type and *drp2a* and *drp2b* mutant leaves by qRT-PCR (Fig. 1A and B). Interestingly, expression levels of *DRP2B* in *drp2a* and *DRP2A* in *drp2b* were 1.3 and 2 times higher, respectively, than those in the wild-type, as if

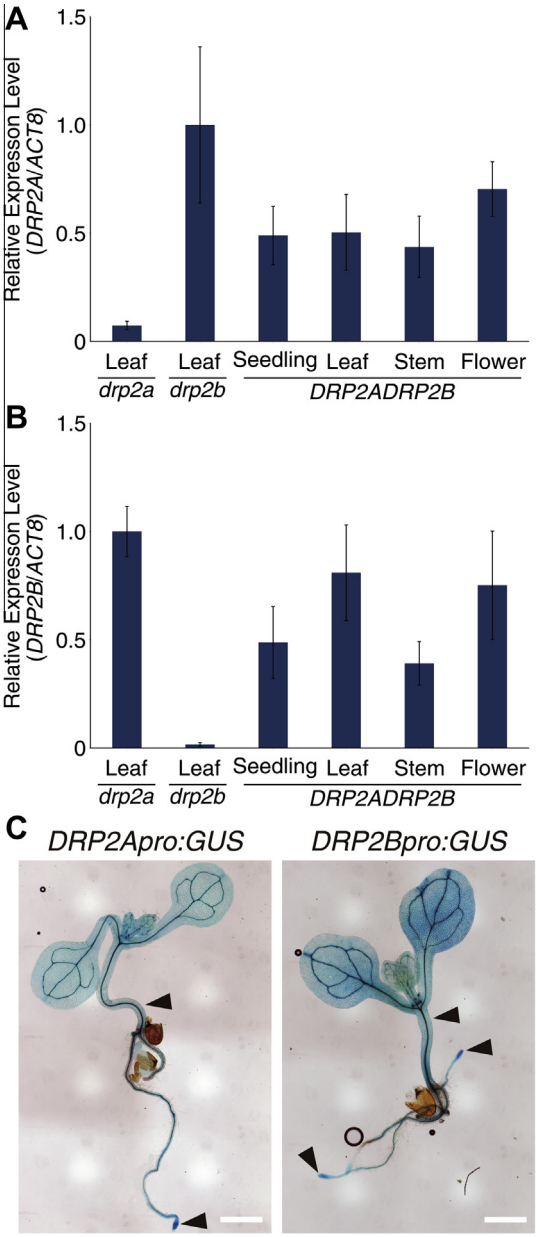

Fig. 1. Spatial expression patterns of *DRP2A* and *DRP2B* in *A. thaliana*. (A,B) qRT-PCR analysis of *DRP2A* (A) and *DRP2B* (B) transcripts in different organs of *A. thaliana* plants. Data represent means ± S.D. (C) Histochemical staining of 10-day-old *A. thaliana* seedlings expressing GUS under the control of *DRP2A* and *DRP2B* promoters. Arrows and arrowheads indicate root apical meristems and vascular bundles, respectively. Bars = 1 mm.

one gene was up-regulated to mitigate the loss of the other. These results indicate that our qRT-PCR system is able to specifically detect each mRNA amount of *DRP2A* and *DRP2B*.

DRP2A and *DRP2B* mRNAs were detected in 10-day-old seedlings, leaf, stem, and flower. GUS signals of *DRP2A* and *DRP2B* promoters were detected ubiquitously in 10-day-old seedlings, especially strong in root apical meristems and vascular bundles (Fig. 1C). These results suggest that *DRP2A* and *DRP2B* have similar spatial expression patterns *in planta*.

3.2. DRP2A and DRP2B interact with each other

To examine whether DRP2A and DRP2B interact with each other, yeast two-hybrid (Y2H) assay among DRP2A, DRP2B and

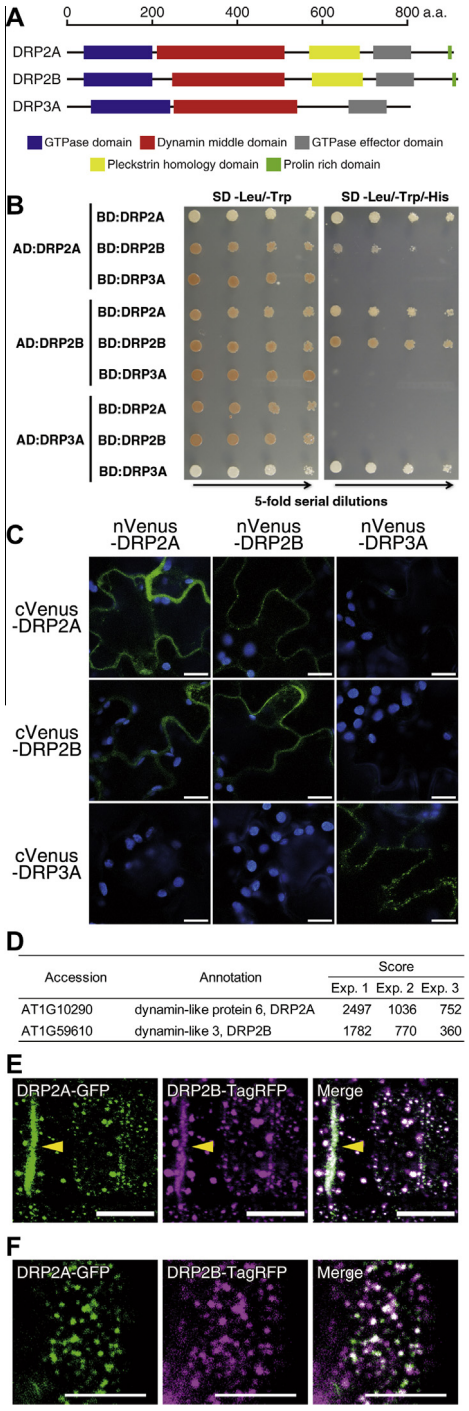

Accession	Annotation	Score		
		Exp. 1	Exp. 2	Exp. 3
AT1G10290	dynamin-like protein 6, DRP2A	2497	1036	752
AT1G59610	dynamin-like 3, DRP2B	1782	770	360

Fig. 2. Interaction and co-localization between DRP2A and DRP2B. (A) Domain structures of DRP2A, DRP2B and DRP3A depicted by PFAM program (http://pfam.sanger.ac.uk). (B) Y2H experiment with DRP2A, DRP2B and DRP3A. Yeast transformants harboring paired constructs for fusion proteins with GAL4 activation domain (AD) and DNA binding domain (BD) were spotted onto a SD/-Leu/-Trp plate (left) and SD/-Leu/-Trp/-His plate (right). (C) BiFC assay showing the interactions among DRP2A, DRP2B and DRP3A. Each panel represents CLSM images of *N. benthamiana* expressing pairs of nVenus and cVenus fusions of DRP2A, DRP2B and DRP3A. Bars = 20 μm. (D) DRP2A and DRP2B proteins identified by mass spectrometry in DRP2A-GFP co-immunoprecipitates. Scores from the three independent experiments were calculated by Mascot (Matrix Science). (E) CLSM images of *A. thaliana* root epidermal cells expressing DRP2A-GFP (green) and DRP2B-TagRFP (magenta). Arrowhead indicates cell plate. Bar = 10 μm. (F) VIAFM images of *A. thaliana* root epidermal cells expressing DRP2A-GFP (green) and DRP2B-TagRFP (magenta). Bar = 5 μm.

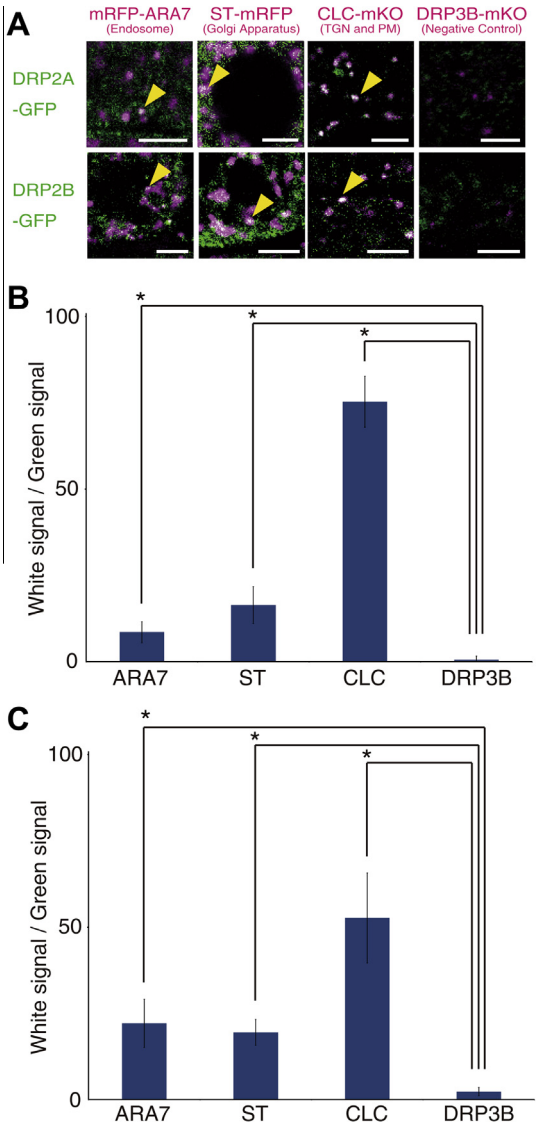

Fig. 3. Intracellular localizations of DRP2A and DRP2B. (A) CLSM images of *A. thaliana* root epidermal cells expressing DRP2A-GFP or DRP2B-GFP (green) and mRFP-tagged markers for post-Golgi organelles (magenta). Arrowheads indicate co-localization sites of GFP and mRFP signals. Bar = 5 μm. (B and C) The percentage of DRP2A-GFP (B) and DRP2B-GFP (C) signals overlapped with mRFP signals in total GFP signals, calculated from three 225 μm^2 CLSM images. Data represent means ± S.D. $^*P < 0.05$. Student's *t*-test.

DRP3A was conducted. DRP3A shows the different domain organization from DRP2A and DRP2B, and was reported to participate in mitochondria fission [19] (Fig. 2A). In results, the interactions between DRP2A-DRP2A, DRP2B-DRP2B and DRP2A-DRP2B were detected (Fig. 2B). Despite the detection of the interaction between DRP3A-DRP3A, which was reported previously [14], the interactions between DRP2A-DRP3A and DRP2B-DRP3A were not found (Fig. 2B). In bi-molecular fluorescent complementation (BiFC) assay, Venus signals were detected *N. benthamiana* leaves transiently expressing nVenus and cVenus combinations of DRP2A and DRP2B (Fig. 2C), confirming that DRP2A and DRP2B interacted with each other and with themselves.

Moreover, we conducted co-immunoprecipitation mass spectrometry (CoIP-MS) analysis with *A. thaliana* seedlings. DRP2A and DRP2B were identified from co-immunoprecipitates with anti-GFP antibody from transgenic plants expressing DRP2A-GFP (Fig. 2D), but not from those expressing GFP only. These results

indicate that DRP2A and DRP2B directly interact with themselves and with each other in *A. thaliana*.

3.3. DRP2A and DRP2B co-localize with each other

In confocal laser scanning microscopy (CLSM) images, almost all GFP and TagRFP signals co-localized in dot-shaped structures (Fig. 2E) and on the cell plate (Fig. 2E, arrowhead). In variable incidence angle fluorescent microscopy (VIAFM) images, almost all GFP and TagRFP also co-localized in dot-shaped foci with 200–500 nm diameters, although the intensity of GFP and TagRFP signals in each focus is uneven. These results indicate that DRP2A and DRP2B are co-expressed and co-localize at dot-shaped organelles, the PM, and the cell plate in *A. thaliana* root epidermal cells.

3.4. DRP2A and DRP2B localize to various post-Golgi organelles

In CLSM images of *A. thaliana* root epidermal cells, DRP2A-GFP and DRP2B-GFP signals largely co-localized with a marker for TGN and the PM (CLC-mKO) [20] and partially co-localized with markers for endosomes (mRFP-ARA7) [21] and Golgi apparatus (ST-mRFP) [22] (Fig. 3A, arrowheads). The co-localizations were significantly stronger than those with DRP3B-mKO signals indicating tips and fission sites of mitochondria [14], which were used as negative controls (Fig. 3B). These results indicate that DRP2A and DRP2B mainly localize to clathrin-labeled compartments within the post-Golgi organelles, including endosomes, Golgi apparatus, TGN and the PM.

3.5. Cytoskeleton and phosphatidylinositol 3- or 4-kinase are required for DRP2 dynamics on the PM

It is expected that inhibitors of cytoskeletal polymerization and/or phosphatidylinositol metabolism would affect the assembly and disassembly of DRP2 on the PM. To evaluate the mobility of DRP2A and DRP2B on the PM, we superimposed DRP2A-GFP or DRP2B-GFP images in the first frame (labeled in green) and the last frame (labeled in red) of time-lapse VIAFM movies covering 15-s observations (Fig. 4). In superimposed images, green foci represent DRP2A-GFP or DRP2B-GFP signals that exist in the first-frame images (t = 0 s), but disappeared in the course of the 15-s VIAFM observation (arrowhead in Fig. 4A). Red foci represent

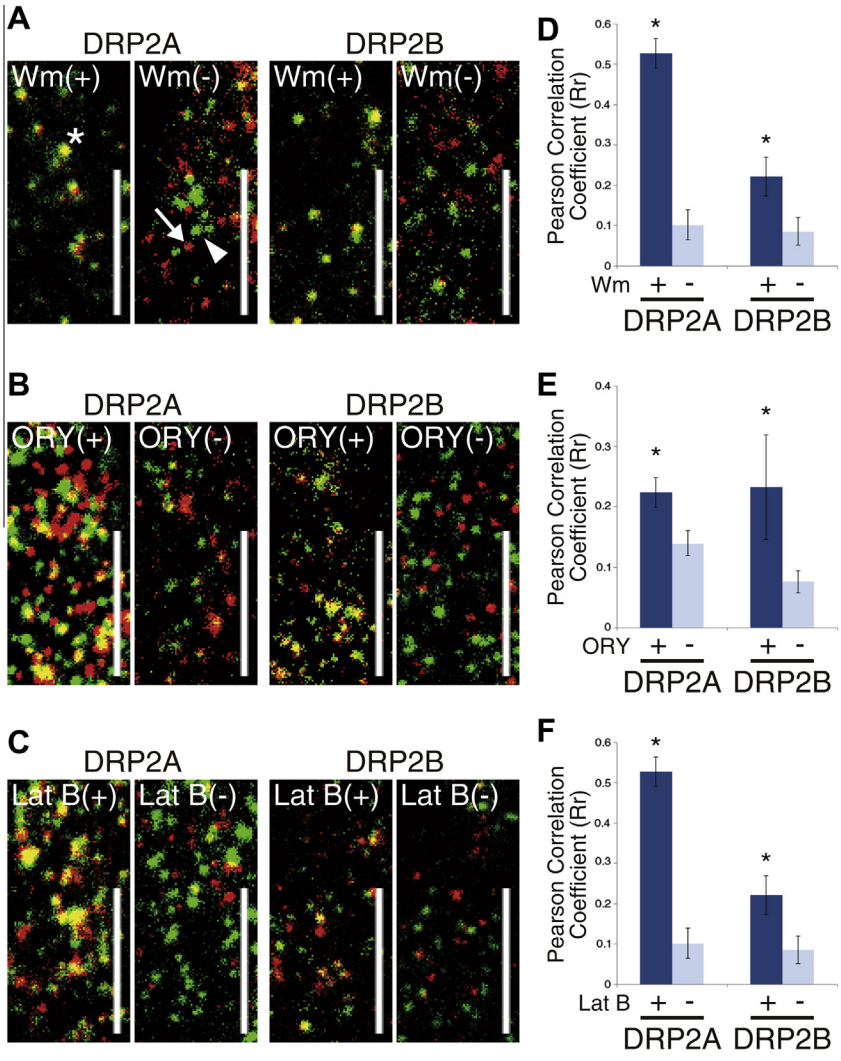

Fig. 4. Effects of PI3/4 K and cytoskeletal inhibitors on the spatiotemporal distribution of DRP2A and DRP2B on the PM. (A–C) VIAFM images of *A. thaliana* root epidermal cells expressing DRP2A- or DRP2B-GFP, acquired at 0 s (green) and 15 s (red) after 2 h treatment with wortmannin (Wm) (A) and 1 h treatment with oryzalin (ORY) (B) and latrunculin B (Lat B) (C). The two images from different time points are merged into single images. Bars = 5 μm. (D–F) Spatial distribution changes between DRP2A- or DRP2B-GFP foci in VIAFM images acquired at 0 s and 15 s. Blue and light blue bars represent the means of Pearson's correlation coefficient (Rr) calculated from eight 81 μm^2 VIAFM images with or without the treatments of Wm (D), ORY (E), and Lat B (F), respectively. Data represent means ± S.D. $^*P < 0.05$. Student's t-test.

DRP2A-GFP or DRP2B-GFP signals that do not exist in the first frame but appeared over the course of the VIAFM observation (arrow in Fig. 4A). Yellow foci represent DRP2A-GFP or DRP2B-GFP signals that stayed in the same place (did not appear or disappear) during the course of the VIAFM observation (asterisk in Fig. 4A). Compared to controls (DMSO treatments), wortmannin (Wm: an inhibitor of phosphatidylinositol 3- and 4- kinases (PI3 K and PI4 K)), oryzalin (ORY: an inhibitor of microtubule polymerization) and latrunculin B (Lat B: an inhibitor of actin polymerization) markedly decreased the number of green and red foci and increased the number of yellow foci, (Fig. 4A–F). The results indicate that these inhibitors significantly decreased the appearing and disappearing mobilities and increased the resident times of DRP2A-GFP and DRP2B-GFP foci on the PM. In addition, Wm decreased the number of DRP2A-GFP and DRP2B-GFP foci in 81 μm^2 VIAFM image (averages of eight images are 44.8 ± 17.2 and 49.1 ± 7.3, respectively) compared to DMSO (81.2 ± 11.7 and 58.4 ± 9.4, respectively) (Fig. 4A). These results indicate that PI3 K or PI4 K activities and actin and tubulin polymerization are required for play important roles in the assembly and disassembly of DRP2A and DRP2B on the PM.

4. Discussion

4.1. DRP2A and DRP2B function redundantly in planta

The results of our study demonstrated that DRP2A and DRP2B interact and co-localize with each other. These findings strongly indicated that DRP2A and DRP2B assemble into homo- and hetero-polymer to function in post-Golgi trafficking. Our results also demonstrated that *DRP2A* and *DRP2B* are expressed constitutively in almost all tissues, although the expressions are strongest in vascular bundles and root apical meristems. *drp2a* or *drp2b* single mutants show no detectable phenotypes [11], while single mutants of genes encoding DRP1 family proteins have clear phenotypes [7]. These results suggest that the two *DRP2* paralogues in *A. thaliana* are functionally redundant *in planta*.

4.2. DRP2 localizes to a wide range of post-Golgi organelles

Our microscopic observations revealed that both DRP2A and DRP2B co-localize with various markers for post-Golgi compartments, most of which are labeled by clathrin. These findings are consistent with previous reports showing the multiple localization of DRP2 to some post-Golgi organelles including the PM [6,10], TGN [23,24], and the forming edge of the cell plate [9]. Interestingly, animal dynamin also localizes to the PM, TGN, and endosomes, and is assumed to participate in clathrin-coated vesicle formation [1]. Hence, the similarity between the intracellular localizations of DRP2 and dynamin raises the possibility that DRP2 takes part in clathrin-mediated trafficking across the wide range of post-Golgi organelles.

We also demonstrated that an inhibitor of PI3 K and PI4 K (wortmannin) affects DRP2 dynamics on the PM. The PH domain of DRP2 has been reported to interact with several kinds of phosphoinositides (PIs) distributed among the post-Golgi organelles: PtdIns3P (endosomes, prevacuolar compartment, and vacuole), PtdIns4P (Golgi apparatus, TGN, and the PM), PtdIns(4,5)P_2 (the PM) [11,24,25]. The affinity of the PH domain for multiple PIs may underlie the broad spectrum of DRP2 localization to post-Golgi organelles. The dynamics of DRP2 on the PM is also affected by inhibitors of tubulin and actin polymerization (oryzalin and latrunculin B). The PRD of DRP2A has been reported to interact with an SH3 domain-containing protein, AtSH3P3, whose animal orthologues help to recruit dynamin to the neck of coated-pits in an actin-dependent manner [26]. However, in plant cells, it is unclear how cytoskeleton regulates the localizations of DRP2. Further studies are needed to identify and determine the function of proteins that interact with DRP2. Such studies should help to unravel the plant-unique mechanism by which vesicles are formed in post-Golgi trafficking.

Acknowledgments

We thank Dr. Akihiko Nakano (RIKEN and The University of Tokyo), Dr. Takashi Ueda (The University of Tokyo), Dr. Tomohiro Uemura (The University of Tokyo) and Dr. Keiko Shoda (RIKEN), for access to LSM780 and kindly donating plant's seeds of mRFP-ARA7 and ST-mRFP. This research was supported by funding to N.T. from grants-in-aid from the Ministry of Education, Culture, Sports, Science and Technology of Japan (Grants 21248002 and 24248001). J.H. was supported by Research Fellowships of the Japan Society for the Promotion of Science for Young Scientists (26 1701).

Appendix A. Supplementary data

Supplementary data associated with this article can be found, in the online version, at http://dx.doi.org/10.1016/j.bbrc.2014.11.065.

References

[1] G.J.K. Praefcke, H.T. McMahon, The dynamin superfamily: universal membrane tubulation and fission molecules?, Nat Rev. Mol. Cell Biol. 5 (2004) 133–147.
[2] J. Hu, Y. Shibata, P.-P. Zhu, C. Voss, N. Rismanchi, W.A. Prinz, T.A. Rapoport, C. Blackstone, A class of dynamin-like GTPases involved in the generation of the tubular ER network, Cell 138 (2009) 549–561.
[3] S. Sever, Dynamin and endocytosis, Curr. Opin. Cell Biol. 14 (2002) 463–467.
[4] S.L. Schmid, V.A. Frolov, Dynamin: functional design of a membrane fission catalyst, Annu. Rev. Cell Dev. Biol. 27 (2011) 79–105.
[5] Z. Hong, S.Y. Bednarek, E. Blumwald, I. Hwang, G. Jurgens, D. Menzel, K.W. Osteryoung, N.V. Raikhel, K. Shinozaki, N. Tsutsumi, D.P.S. Verma, A unified nomenclature for *Arabidopsis* dynamin-related large GTPases based on homology and possible functions, Plant Mol. Biol. 53 (2003) 261–265.
[6] M. Fujimoto, S. Arimura, T. Ueda, H. Takanashi, Y. Hayashi, A. Nakano, N. Tsutsumi, Arabidopsis dynamin-related proteins DRP2B and DRP1A participate together in clathrin-coated vesicle formation during endocytosis, Proc. Natl. Acad. Sci. U.S.A. 107 (2010) 6094–6099.
[7] S.Y. Bednarek, S.K. Backues, Plant dynamin-related protein families DRP1 and DRP2 in plant development, Biochem. Soc. Trans. 38 (2010) 797–806.
[8] J. Mravec, J. Petrášek, N. Li, S. Boeren, R. Karlova, S. Kitakura, M. Pařezová, S. Naramoto, T. Nodzyński, P. Dhonukshe, S.Y. Bednarek, E. Zažímalová, S. de Vries, J. Friml, Cell plate restricted association of DRP1A and PIN proteins is required for cell polarity establishment in *Arabidopsis*, Curr. Biol. 21 (2011) 1055–1060.
[9] M. Fujimoto, S. Arimura, M. Nakazono, N. Tsutsumi, Arabidopsis dynamin-related protein DRP2B is co-localized with DRP1A on the leading edge of the forming cell plate, Plant Cell Rep. 27 (2008) 1581–1586.
[10] N.G. Taylor, A role for Arabidopsis dynamin related proteins DRP2A/B in endocytosis; DRP2 function is essential for plant growth, Plant Mol. Biol. 76 (2011) 117–129.
[11] S.K. Backues, D.a. Korasick, A. Heese, S.Y. Bednarek, The Arabidopsis dynamin-related protein2 family is essential for gametophyte development, Plant Cell 22 (2010) 3218–3231.
[12] S. Miyagishima, H. Kuwayama, H. Urushihara, H. Nakanishi, Evolutionary linkage between eukaryotic cytokinesis and chloroplast division by dynamin proteins, Proc. Natl. Acad. Sci. U.S.A. 105 (2008) 15202–15207.
[13] T. Murashige, F. Skoog, A revised medium for rapid growth and bio assays with tobacco tissue cultures, Physiol. Plant. 15 (1962) 473–497.
[14] M. Fujimoto, S. Arimura, S. Mano, M. Kondo, C. Saito, T. Ueda, M. Nakazono, A. Nakano, M. Nishimura, N. Tsutsumi, Arabidopsis dynamin-related proteins DRP3A and DRP3B are functionally redundant in mitochondrial fission, but have distinct roles in peroxisomal fission, Plant J. 58 (2009) 388–400.
[15] M. Karimi, D. Inzé, A. Depicker, GATEWAY™ vectors for Agrobacterium-mediated plant transformation, Trends Plant Sci. 7 (2002) 193–195.
[16] S. Nakamura, S. Mano, Y. Tanaka, M. Ohnishi, C. Nakamori, M. Araki, T. Niwa, M. Nishimura, H. Kaminaka, T. Nakagawa, Y. Sato, S. Ishiguro, Gateway binary vectors with the bialaphos resistance gene, bar, as a selection marker for plant transformation, Biosci. Biotechnol. Biochem. 74 (2010) 1315–1319.
[17] C. Gehl, R. Waadt, J. Kudla, R.-R. Mendel, R. Hänsch, New GATEWAY vectors for high throughput analyses of protein-protein interactions by bimolecular fluorescence complementation, Mol. Plant. 2 (2009) 1051–1058.
[18] M. Fujiwara, T. Uemura, K. Ebine, Y. Nishimori, T. Ueda, A. Nakano, M.H. Sato, Y. Fukao, Interactomics of Qa-SNARE in *Arabidopsis thaliana*, Plant Cell Physiol. 55 (2014) 781–789.

[19] S. Arimura, G.P. Aida, M. Fujimoto, M. Nakazono, N. Tsutsumi, Arabidopsis dynamin-like protein 2a (ADL2a), like ADL2b, is involved in plant mitochondrial division, Plant Cel Physiol. 45 (2004) 236–242.
[20] E. Ito, M. Fujimoto, K. Ebine, T. Uemura, T. Ueda, A. Nakano, Dynamic behavior of clathrin in *Arabidopsis thaliana* unveiled by live imaging, Plant J. 69 (2012) 204–216.
[21] K. Ebine, M. Fujimoto, Y. Okatani, T. Nishiyama, T. Goh, E. Ito, T. Dainobu, A. Nishitani, T. Uemura, M.H. Sato, H. Thordal-Christensen, N. Tsutsumi, A. Nakano, T. Ueda, A membrane trafficking pathway regulated by the plant-specific RAB GTPase ARA6, Nat. Cell Biol. 13 (2011) 853–859.
[22] T. Uemura, Y. Suda, T. Ueda, A. Nakano, Dynamic behavior of the *trans*-golgi network in root tissues of *Arabidopsis* revealed by super-resolution live imaging, Plant Cell Physiol. 55 (2014) 694–703.
[23] J.B. Jin, Y.A. Kim, J. Kim, H. Lee, H. Kim, G. Cheong, I. Hwang, A new dynamin-like protein, ADL6, is involved in trafficking from the trans-Golgi network to the central vacuole in arabidopsis, Plant Cell 13 (2001) 1511–1525.
[24] B.C.-H. Lam, T.L. Sage, F. Bianchi, E. Blumwald, Regulation of ADL6 activity by its associated molecular network, Plant J. 31 (2002) 565–576.
[25] S.H. Lee, J.B. Jin, J. Song, M.K. Min, D.S. Park, Y.-W. Kim, I. Hwang, The intermolecular interaction between the PH domain and the C-terminal domain of Arabidopsis dynamin-like 6 determines lipid binding specificity, J. Biol. Chem. 277 (2002) 31842–31849.
[26] H.S. Shpetner, J.S. Herskovits, R.B. Vallee, A binding site for SH3 domains targets dynamin to coated pits, J. Biol. Chem. 271 (1996) 13–16.